ESKİŞEHİR TECHNICAL UNIVERSITY JOURNAL OF SCIENCE AND TECHNOLOGY
A- APPLIED SCIENCES AND ENGINEERING

2020, 21(4), pp. 539-553, DOI: 10.18038/estubtda.755217

RESEARCH ARTICLE

GAMMA RADIATION SHIELDING PROPERTIES OF NATURAL GLASS OBSIDIAN

Gülçin BİLGİCİ CENGİZ [1], İlyas ÇAĞLAR [2,*], Gökhan BİLİR [1]

[1] Department of Physics, Faculty of Arts and Sciences, Kafkas University, 36100 Kars, Turkey
[2] Kazım Karabekir Vocational School of Technical Sciences, Department of Electricity and Energy, Kafkas University, 36100 Kars, Turkey

ABSTRACT

The present study was carried out to estimate gamma radiation shielding properties of natural glass obsidian. For this purpose, linear attenuation coefficient, mass attenuation coefficient, mean free path, half-value layer, tenth-value layer, effective atomic number and effective electron number values of obsidian samples in black and brown colors were experimentally measured for 661.66, 1172.23 and 1332.48 keV gamma ray energies obtained from ^{137}Cs, and ^{60}Co radioactive sources. Measurements were performed at narrow-beam transmission geometry using a NaI(Tl) scintillation detector. In addition, all these parameters were theoretically calculated by using WinXCOM program in the energy region of 0.015 to 15 MeV. A good agreement was observed between theoretical and experimental values. Furthermore, energy absorption and exposure buildup factors (EABF and EBF) of obsidian specimens were determined in the energy range of 0.015 to 15 MeV using G-P fitting method. Finally, it can be concluded that these naturally occurring volcanic glasses can be used for radiation shielding applications.

Keywords: Gamma Radiation, Mass attenuation coefficient, Obsidian, G-P fitting method, Buildup factors

1. INTRODUCTION

Over the past few years, growing attention in proper designs for radiation protection has raised up due to the increased use of radiation in various fields such as science, technology, industry, agriculture, medicine, radiation biophysics, radiation protection, and the like [1,2]. Many researchers have focused on the design of barrier materials that reduce or retain X and gamma rays to protect both humans and their environment from the harmful impacts of radiation. Mass attenuation coefficients (μ_m), linear attenuation coefficients (μ) mean free path (mfp), half value layer (HVL), tenth value layer (TVL), effective atomic number (Z_{eff}), effective electron number (N_{eff}), energy absorption and exposure buildup factors (EABF and EBF) are basic qualities that shows the radiation shielding effectiveness of any materials [3].

Extensive surveys have been performed on investigation of radiation shielding features of various materials such as steels, alloys, superconductors, various ores concrete and etc. [4-14]. Moreover, there are several theoretical and experimental studies have been carried out to estimate radiation attenuation behaviors of various glass system. For example, Singh et al. experimentally determined μ_m, Z_{eff} and N_{eff} values of $xCaO•(0.3-x)SrO•0.7B_2O_3$ glass system in the gamma ray energy range 511–1332 keV and compared with theoretical values obtained from WinXCOM program [15, 16]. The radiation shielding parameters (μ_m, MFP, Z_{eff} and N_{eff}) of the borosilicate glasses were theoretically computed using WinXCOM program by Chanthima and Kaewkhao [17]. The μ_m, Z_{eff} and N_{eff} of WO_3 based glass system were experimentally determined for the 0.356 and 0.662 MeV energies and theoretically calculated at 1 keV-100 GeV using XCOM program by Mostafa et al. [18]. Sayyed et al. theoretically investigated gamma ray attenuation behaviors of different germanate glasses in the energy range of 15 keV to 10 MeV by using WinXCOM program [19]. Ahmed et al. experimentally measured different gamma ray attenuation parameters (μ, μ_m and HVL) of some sodium iron phosphate glasses at the energy range of 121.8 keV to 1407.9 keV [20].

*Corresponding Author: ilyas.caglar@kafkas.edu.tr
Received: 19.06.2020 Published: 28.12.2020

Obsidian, also called volcanic glass, is a type of alumino-silicate glass that contains iron impurities and some tiny particles (particle-dispersed glasses). It is an amorphous volcanic glass which have glassy brightness and is found in nature in black, gray, brown, red and green colors [21]. The chemical compositions of the studied obsidian are taken from the literature [22] and given in Table 1. When the main oxide contents of the both obsidian glasses evaluated, it is seen that they are rich in SiO_2 and alkalis ($Na_2O + K_2O > 8\%$). The Na_2O content of each obsidian sample is higher than the K_2O content. As can be seen in Table 1, there is no significant difference in the main oxide contents of two samples and they have similar chemical composition in general terms. So far, there is not enough information in the literature about the radiation protection properties of this natural glass.

Table 1. Chemical composition of obsidian samples [22]

Sample	SiO_2	TiO_2	AI_2O_3	Fe_2O_3	MnO	MgO	CaO	Na_2O	K_2O	P_2O_5
Black Obsidian **(BKO)**	75,80	0,10	13,00	1,67	0,10	0,10	0,47	4,77	3,97	< 0.1
Brown Obsidian **(BNO)**	75,65	0,10	12,90	1,85	0,10	0,10	0,55	4,45	4,20	< 0.1

The objectives of this present study was to estimate the gamma ray attenuation parameters such as μ, μ_m mfp, HVL, TVL, Z_{eff} and N_{eff} in black and brown color obsidian specimens which were collected from Sarıkamış located in Turkey These parameters were measured for 661.66, 1173.24 and 1332.48 keV photons obtained from ^{137}Cs and ^{60}Co point sources and the theoretical values of these parameters were calculated using the WinXCOM computer program. Besides these parameters EABF and EBF values were calculated at the 0.015 to 15 MeV energy range. The obtained experimental values for obsidian samples compared with the results of WinXCOM calculations. In addition, the radiation shielding capabilities of investigated naturally occurring volcanic glasses were investigated.

2. MATERIALS AND METHODS

Obsidian specimens were taken from Sarıkamış district of Kars province located at the eastern part of Turkey. The obtained samples were cut in a diameter of 18 mm and 5mm thickness using glass cutting machine to perform mass attenuation coefficient measurements. The prepared obsidian samples were irradiated with 661.66 keV gamma ray energy emitted from the ^{137}Cs point source, 1173.23 and 1332.48 keV gamma ray energies from the ^{60}Co point source.

A 3inch × 3 inch NaI(Tl) detector based on a gamma-ray spectrometer was employed to evaluate the unattenuated (I_0) and attenuated (I) photon intensities (Figure 1). The theoretical μ_m values for the prepared obsidian specimens were determined using WinXCOM software package [16]. Each spectrum was counted for a period of 600 s and repeated 3 times for both samples to obtain accurate measurement results. Maestro is a multi-channel analyzer (MCA) emulation software package from Ortec Company. The spectrum analyzed using an MCA system and Maestro based PC (Personal Computer) [23]. The typical spectra obtained from ^{137}Cs and ^{60}Co radioactive sources (for 661.66 keV, 1173.23 keV and 1332.48 keV) without attenuation and attenuated by present brown and black obsidian are given in Figure 2 (a and b). The μ_m values of obsidian specimens at different energies were experimentally determined using Lambert-Beer law given by equation 1 [12].

$$I = I_0 e^{-(\frac{\mu}{\rho})t} \quad (1)$$

where, $\mu/\rho = \mu_m$ is the mass attenuation coefficient in cm^2/g, ρ is the density in g/cm^3, t is sample mass thickness (the mass per unit area) in g/cm^2, I_0 and I are the incident and attenuated photon intensity, respectively.

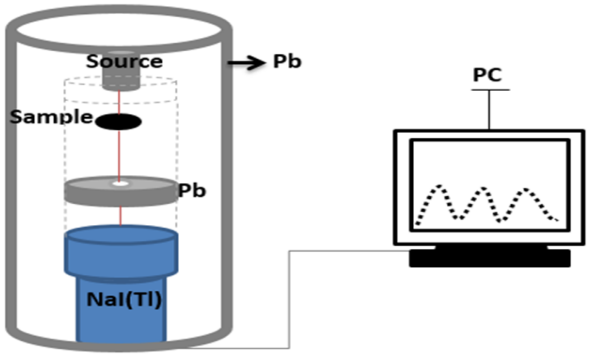

Figure 1. Experimental setup

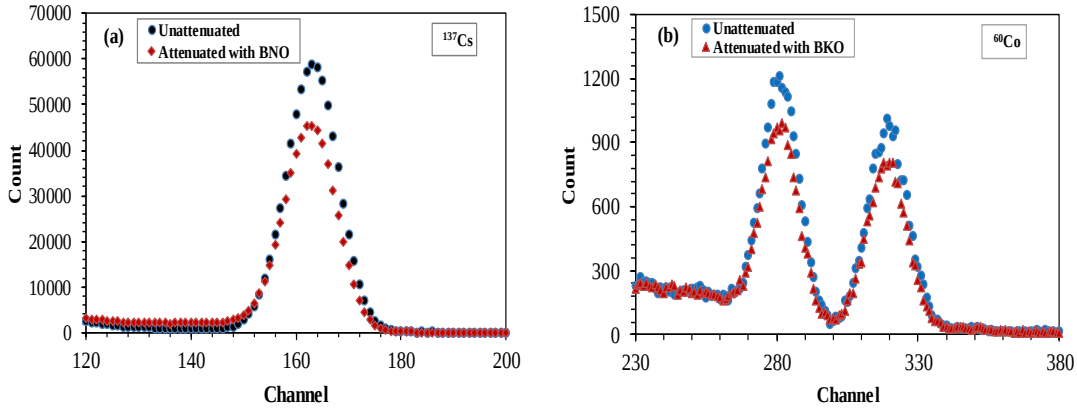

Figure 2. The typical attenuated and unattenuated γ-ray spectrum of (a) ^{137}Cs, (b) ^{60}Co

2.1. Calculations

The theoretical μ_m values for any compound or mixture containing various elements is given by mixture rule [24]:

$$\mu_m = \frac{\mu}{\rho} = \sum_i w_i (\mu_m)_i \tag{2}$$

where w_i and $(\mu_m)_i$ are the weight fraction and mass attenuation coefficient for individual element in mixture, respectively. mfp which is the inverse of μ denotes the average distance between two successive interactions of photons and is calculated by the following formula [5, 25]:

$$mfp = \frac{1}{\mu} \tag{3}$$

where, μ indicates the linear attenuation coefficient of absorber. A widely used important radiation shielding parameter (reflecting effectiveness of radiation protection for any materials) called half value layer is described as the sample thickness which reduces photon intensity to 50% of incident intensity and it can be computed according to following expression [19, 26]:

$$HVL = \frac{0.693}{\mu} \tag{4}$$

Tenth value layer (TVL) in units of cm can be obtained by using following expression [5]:

$$TVL = \frac{\ln(10)}{M} \tag{5}$$

The total atomic cross-sections in unit of barns/atom for investigated samples were computed using μ_m values through the following expression [4, 25]:

$$\sigma_a = \frac{\mu_m}{N_A \sum_i \frac{w_i}{A_i}} \tag{6}$$

where N_A is the Avogadro constant, A_i and w_i are atomic and fractional weights of the ith element respectively. The total electronic cross-section, (σ_e), can be calculated according to equation 7 [7, 11].

$$\sigma_e = \frac{1}{N_A} \sum_i \frac{f_i A_i}{Z_i} (\mu_m)_i = \frac{\sigma_a}{Z_{eff}} \tag{7}$$

where f_i and Z_i are the fractional abundance and atomic number of the ith element respectively. The effective atomic number (Z_{eff}) represents the weighted average atomic number of the material consisting of different elements and can be obtain by using the following expression [3-5, 25]:

$$Z_{eff} = \frac{\sigma_a}{\sigma_e} \tag{8}$$

The effective electron number or electron density (N_{eff}), described as the number of electrons which interacted with photon per unit mass can be determined using μ_m and σ_e values with the help of the following practical formula [3, 5, 25].

$$N_{eff} = \frac{\mu_m}{\sigma_e} \tag{9}$$

To compute EABF and EBF of obsidian glasses under the study, firstly equivalent atomic number (Z_{eq}) for specimens were calculated in the energy range 0.015–15 MeV using the ratio of Compton partial mass attenuation coefficient to total mass attenuation coefficient (R; $(\mu_m)_{Compton}$ / $(\mu_m)_{Total}$) according to the following formula [13, 27-29];

$$Z_{eq} = \frac{Z_1(\log R_2 - \log R) + Z_2(\log R - \log R_1)}{\log R_2 - \log R_1} \tag{10}$$

where R represents the ratio of $(\mu_m)_{Compton}$ and $(\mu_m)_{Total}$ for an obsidian specimen at a given energy. Z_1 and Z_2 denotes atomic numbers of the elements corresponding to the ratios R_1 and R_2, respectively. More details can be found in Reference [29]. The values of $(\mu_m)_{Compton}$ and $(\mu_m)_{Total}$ at the selected energies were obtained using WinXCOM program for the elements Z = 4–30 and both obsidian specimens. Then, G-P fitting coefficients (a, b, c, d, and X_k) for the specimens were generated by applying a similar interpolation method as given by the equation 12 [8, 28, 29];

$$P = \frac{P_1(\log Z_2 - \log Z_{eq}) + P_2(\log Z_{eq} - \log Z_1)}{\log Z_2 - \log Z_1} \tag{11}$$

where P denotes G-P fitting parameters of studied obsidian specimens. P_1 and P_2 are the values of G-P fitting coefficients corresponding to the Z_1 and Z_2 atomic numbers at a specific energy, respectively. The G-P fitting coefficients for elements were obtained from the ANSI/ANS-6.4.3 database, which provides the G-P fitting parameters for 23 elements (Z=4–92), water, air and concrete in the energy region of 0.015-15 MeV up to 40 mfp [30]. Finally, the computed G-P fitting coefficients were used to compute the EABF and EBF's of obsidian glasses through the below equations [13, 31-33].

$$B(E,X) = 1 + \frac{b+1}{K-1}(K^X - 1) \quad for\ K \neq 1 \tag{12}$$

$$B(E.X) = 1 + (b-1)X \quad for\ K = 1 \tag{13}$$

$$K(E,X) = cx^a + d\frac{\tanh\left(\frac{x}{X_k} - 2\right) - \tanh(-2)}{1 - \tanh(-2)} \quad for\ x \leq 40\ mfp \tag{14}$$

where E, x and K (E, X) are the photon energy, penetration depth in mfp and dose multiplicative factor, respectively. a, b, c, d and X_k are the G-P fitting parameters.

3. RESULTS AND DISCUSSIONS

The mass attenuation coefficient for X and gamma rays is one of the most important quantity in many fields such as radiation physics, radiation dosimetry, biology, medicine, agriculture, industry and etc. [7]. It gives the number of photons scattered or absorbed and depends on the photon energy and the density of the absorber material [11]. The experimental μ_m values of the natural obsidian glasses were measured at the 661.66, 1173.24 and 1332.48 keV photon energies and are summarized in Table 2. The average error in the experimental measurements in Table 2 is less than 6.2% and this error is caused by calculation of the peak area in the spectra, the measurement of the mass thickness of the samples and systematic errors. The measured μ_m values were also compared with the theoretical values obtained by WinXCOM for the same photon energies and displayed in Table 3. As shown in this table, our measured μ_m values are in a good agreement with the theoretically calculated values for obsidian glasses. The obtained μ_m values of obsidian glasses are compared in Table 3 with the reported μ_m values of the different materials for example, BBBG (barium–bismuth–borosilicate glass with the composition of 50BaO–5 Bi_2O_3 45 borosilicate) [34], SIPG (sodium iron phosphate glass with the composition of 15 mole % Na_2O, 15 mole % Fe_2O_3. 70 mole % P_2O_5.5 CdO) [20], and also normal concrete [35]. It observed that the μ_m values of our investigated both obsidians are compatible with the μ_m values of BBG, SIPG and ordinary concrete (OC). For example, the theoretical μ_m values of BBBG, SPIG and OC were 0.0795, 0.041 and 0.0780 cm^2/g at 661.66 keV gamma ray energy. The measured μ_m values of BNO and BKO for same gamma ray energy are similar to the value of BBBG and OC and slightly higher than the value of SPIG. Therefore, these obsidian glasses could be used as radiation shield especially at low energies.

Table 2. The experimental and theoretical mass attenuation coefficients (cm^2/g) for obsidian specimens, BBG SPIG and OC

Energy (keV)	BNO		BKO		BBBG	SIPG	OC
	Exp.	Theo.	Exp.	Theo.	Theo.	Exp.	Theo.
661.66	0.07960 ± 0.00103	0.076891	0.07675± 0.00100	0.076890	0.0795	0.041	0.0780
1173.23	0.05831 ± 0.00462	0.058479	0.05746 ± 0.00459	0.058480	0.0561	0.044	0.0593
1332.48	0.05212 ± 0.00498	0.054789	0.05094 ± 0.00474	0.054790	0.0523	0.034	0.0555

In addition, the variations of experimentally and theoretically mass and linear attenuation coefficients with incident photon energy (0,015-15 MeV) were plotted in Figure 3. (a and b) to show the energy dependence of these parameters.

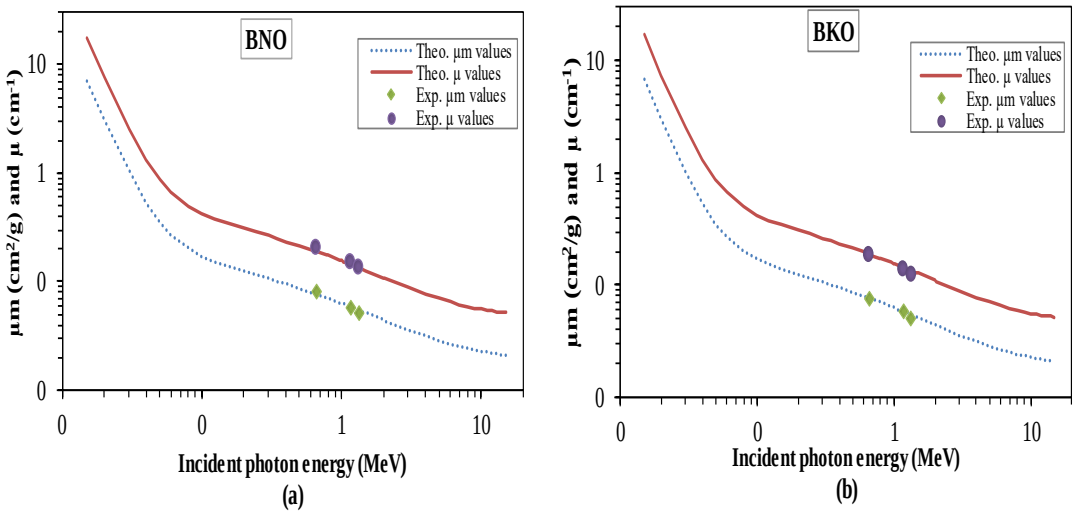

Figure 3. (a, b) μ and μ_m values of (a) brown and (b) black obsidian versus incident photon energy.

As can be seen from the Figure 3, values of both theoretical and experimental μ_m values for investigated samples decreases with increase in the photon energy. As a result of our studies, it was seen that the μ_m and μ values for obsidian specimens decreases rapidly with the increasing of the incident photon energy up to 0.1 MeV. In the moderate energy region (0.1 - 5.0 MeV), these values decrease slowly with the increase of the incident photon energy. At last, in the E > 5 MeV the μ_m and μ values have a very weak dependence of the incident photon energy. This trend can be explained according to different interaction mechanism occurring between photons and material for different energy regions [4]. In the low energy region photoelectric interaction mechanism is dominant process and the photoelectric cross section depends inversely on the energy (i.e. $E^{-3.5}$) and depends upon the atomic number as Z^{4-5}. In intermediate energies Compton Scattering becomes the dominant mechanism and the Compton cross section changes directly with the atomic number Z, and inversely proportional to the photons energy (i.e. E^{-1}). Then, in the high energy region pair production is dominant interaction and the cross-section for pair production depends upon atomic number as Z^2 and logarithmically on energy (log E) [27, 29, 36].

In order to evaluate photon attenuation performance of studied samples mfp, HVL and TVL parameters were determined at photon energies of 0.015–15 MeV using the μ values. The variations of mfp, HVL, and TVL values according to incident photon energy for brown and black obsidians are given in Figure 4 (a and b). It is seen that both the experimental and theoretical values of mfp, HVL and TVL, parameters increase with increasing photon energy. Our obtained trends in the mfp, HVL and TVL parameters are found to be similar with the reported these parameters for some AISI coded stainless steel [5]. At the 661.66, 1172.23 and 1332.48 keV gamma ray energies, the experimental mfp values were measured to be 4.907, 6,699 and 7.495 cm for Brown obsidian, 5.296, 7.074 and 7.980 cm for black obsidian respectively. The experimental HVL values of were measured to be 3.401, 4.633 and 5.195 cm for Brown obsidian, 3.671, 4.904 and 5.532 cm for black obsidian at the same gamma ray energies respectively. The experimental TVL values of were also measured to be 11.299, 15.474 and 17.257 cm for Brown obsidian, 12.195, 16.289 and 18.375 cm for black obsidian at the same gamma ray energies respectively.

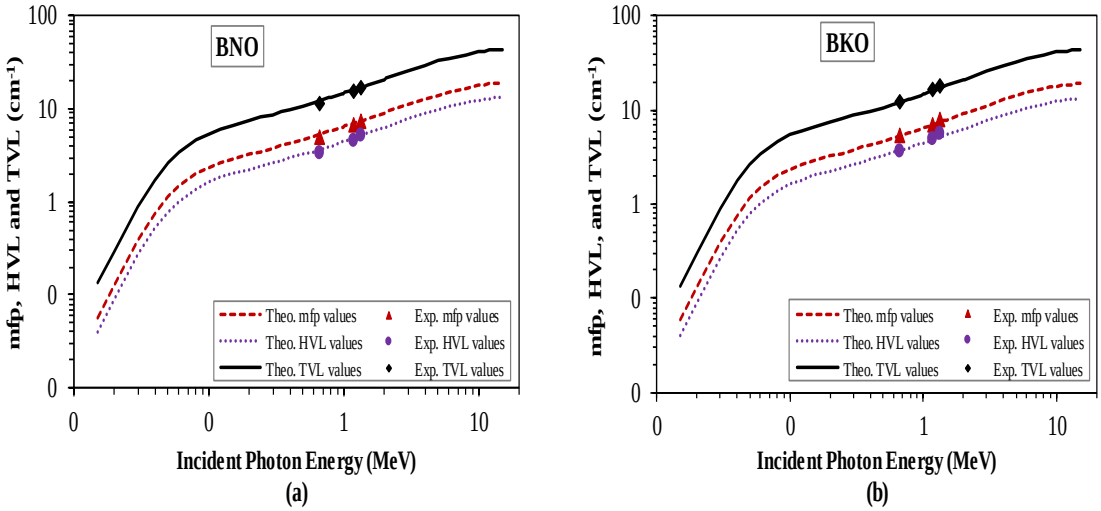

Figure 4. (a, b) mfp, HVL and TVL values of brown and black obsidian versus incident photon energy.

On the other hand, the comparisons of measured and computed mfp, HVL and TVL values of both specimens with the values ordinary concrete are given in Figure 5 (a, b, c). According to these results, the mfp, HVL and TVL values of both specimens for 661.66, 1172.23 are lower than the values OC. At the same time, the experimental mfp, HVL and TVL values of BNO is slightly lower than the values OC for 1332.48 keV. It is seen that mfp, HVL and TVL values of black obsidian slightly higher than the values of brown obsidian, therefore, brown obsidian may be used as a better alternative gamma ray protection material than black obsidian. Because these parameters are commonly used quantities in order to estimate radiation shielding property of any material, having low mfp, HVL and TVL values generally exhibit better shielding features.

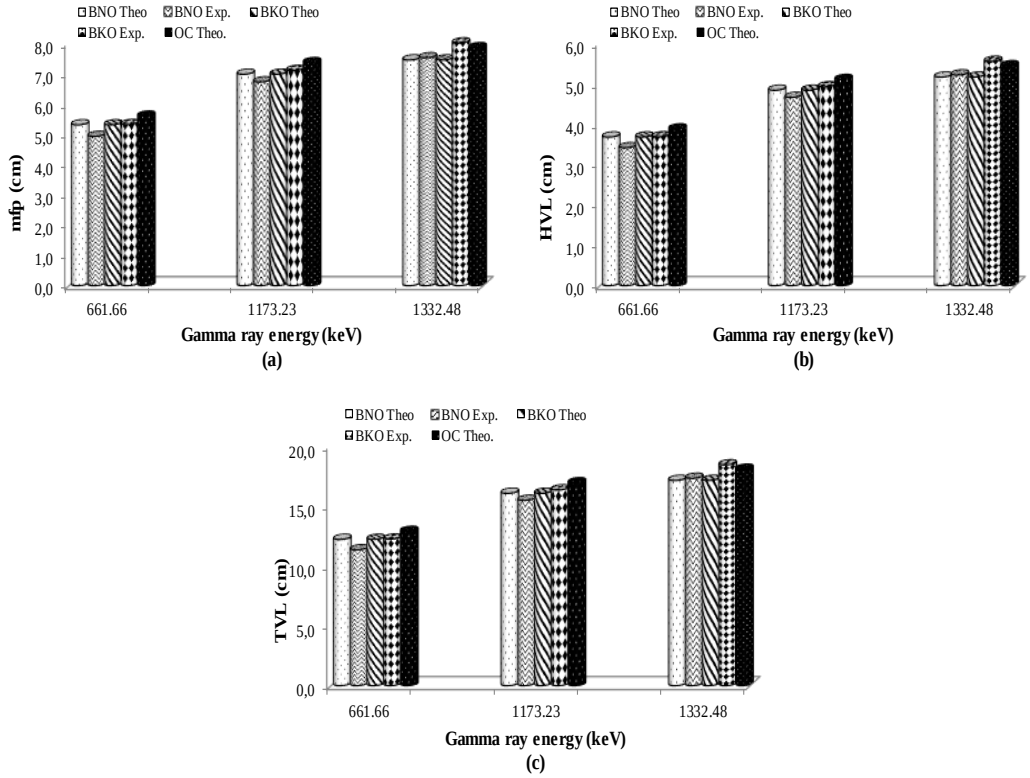

Figure 5. Comparison of mfp HVL and TVL for the investigated samples with OC.

The effective atomic number (Z_{eff}) and effective electron numbers (N_{eff}) for obsidian specimens were calculated at photon energies of 0.015 – 15 MeV using equations 8 and 9, respectively. The variations of these parameters (Z_{eff} and N_{eff}) with the incident photon energy are given in Figure 6 (a and b), respectively. It observed that the measured Z_{eff} and N_{eff} values are consistent with the theoretically calculated values for obsidian glasses at 661.66 and 1173.24 keV, but Z_{eff} and N_{eff} values of both specimens for 1332.48 keV slightly lower than the calculated values. This dissimilarity may be arising from the difference between the measured and calculated μ_m values. Hence Z_{eff} and N_{eff} values of BNO and BKO were compared with the values of OC. It seen that while the Z_{eff} values of both specimens are higher than the OC, N_{eff} values of both specimens are lower than the OC. It is well known that the N_{eff} value for any sample is closely related to the Z_{eff}, therefore variation of N_{eff} with the incident photon energy has a similar tendency to Z_{eff}. Also, one can be seen from Figure 6 (a and b) that the Z_{eff} and N_{eff} values of investigated obsidian specimens decreased with the increasing photon energy at low energies and maximum values of Z_{eff} and N_{eff} are below 0.1 MeV. In the moderate energies (0.1 - 5 MeV) Z_{eff} and N_{eff} have minimum values and started to slowly increase above about 5 MeV. The present trend in the Z_{eff} and N_{eff} values for the obsidian specimens can be understood according to the above mentioned three interaction mechanism between photon and material.

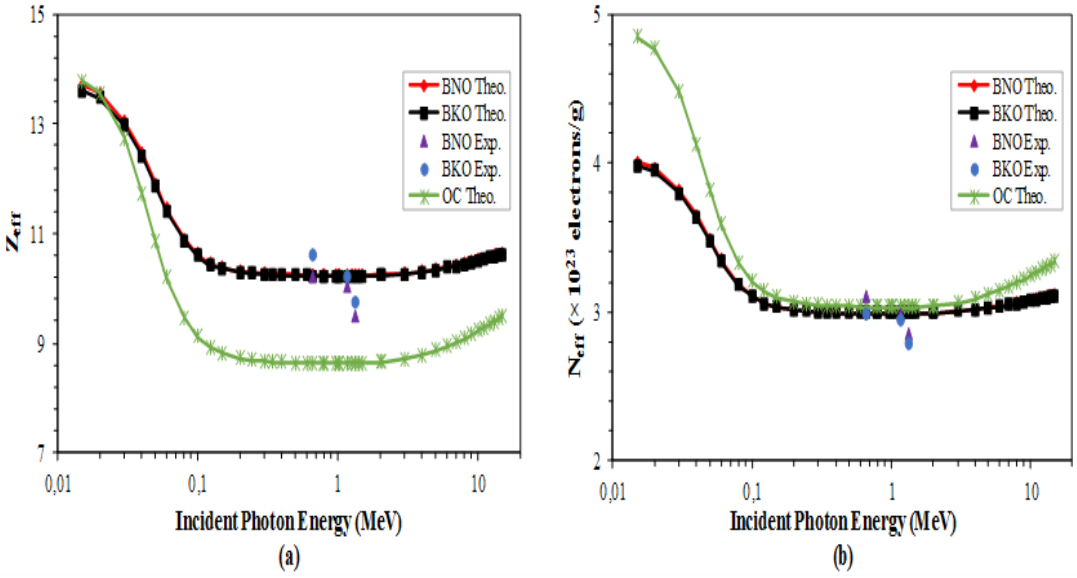

Figure 6. The variations of Z_{eff} and N_{eff} against incident photon energies.

The buildup factors for obsidian samples were determined by using G–P fitting technique for some selected penetration depths (1, 5, 10, 20, 30 and 40 mfp) and in the region of 0.015 to 15 MeV. Table 3 and 4 represent the computed equivalent atomic numbers (Z_{eq}) and G-P fitting coefficients (a, b, c, d and Xk) for EABF and EBF of black and brown obsidian, respectively.

Table 3. Z_{eq} and G-P fitting coefficients for Brown Obsidian.

Energy (MeV)	Z_{eqq}	EABF					EBF				
		a	b	c	d	Xk	a	b	c	d	Xk
0.015	12.269	0.219	1.035	0.391	-0.144	13.549	0.210	1.035	0.399	-0.135	13.935
0.02	12.347	0.205	1.082	0.399	-0.106	14.411	0.193	1.079	0.419	-0.101	14.151
0.03	12.421	0.197	1.265	0.432	-0.106	14.174	0.193	1.260	0.437	-0.103	14.690
0.04	12.451	0.156	1.580	0.527	-0.084	15.089	0.154	1.554	0.532	-0.082	14.990
0.05	12.460	0.138	2.084	0.598	-0.078	14.089	0.113	1.942	0.649	-0.058	15.180
0.06	12.461	0.092	2.617	0.734	-0.065	13.893	0.087	2.336	0.748	-0.057	13.964
0.08	12.437	0.014	3.609	0.999	-0.023	14.243	0.018	2.811	0.988	-0.027	13.382
0.1	12.400	-0.037	4.155	1.229	0.001	12.993	-0.024	2.998	1.180	-0.010	12.573
0.15	12.295	-0.095	4.112	1.545	0.031	13.572	-0.070	2.985	1.425	0.012	17.100
0.2	12.210	-0.113	3.658	1.663	0.039	13.792	-0.085	2.836	1.519	0.018	16.213
0.3	12.089	-0.119	3.060	1.698	0.042	14.178	-0.093	2.594	1.559	0.022	16.892
0.4	12.037	-0.113	2.753	1.647	0.037	14.520	-0.093	2.436	1.539	0.023	15.489
0.5	11.976	-0.107	2.552	1.598	0.037	14.436	-0.089	2.316	1.506	0.024	15.974
0.6	11.924	-0.100	2.415	1.546	0.034	14.579	-0.086	2.223	1.475	0.025	15.290
0.8	11.947	-0.086	2.237	1.450	0.030	14.822	-0.076	2.101	1.402	0.023	15.617
1	11.825	-0.075	2.114	1.380	0.027	15.074	-0.069	2.007	1.351	0.023	15.692
1.5	11.540	-0.053	1.938	1.251	0.020	14.407	-0.049	1.872	1.233	0.017	15.381
2	11.378	-0.035	1.841	1.158	0.013	14.622	-0.034	1.792	1.154	0.012	15.082
3	11.254	-0.010	1.703	1.053	-0.001	11.723	-0.012	1.681	1.058	0.001	12.052
4	11.239	0.008	1.612	0.985	-0.011	13.481	0.006	1.604	0.993	-0.009	12.900
5	11.223	0.021	1.544	0.940	-0.018	12.751	0.018	1.536	0.953	-0.021	14.040
6	11.226	0.024	1.478	0.929	-0.027	15.842	0.029	1.492	0.919	-0.023	11.527
8	11.213	0.033	1.386	0.904	-0.023	12.206	0.033	1.406	0.902	-0.027	13.604
10	11.208	0.034	1.321	0.899	-0.028	14.072	0.043	1.346	0.878	-0.033	13.168
15	11.206	0.042	1.226	0.882	-0.037	14.598	0.062	1.261	0.828	-0.055	14.326

Table 4. Z_{eq} and G-P fitting coefficients for Black Obsidian.

Energy (MeV)	Z_{eqq}	EABF					EBF				
		a	b	c	d	Xk	a	b	c	d	Xk
0.015	12.211	0.217	1.035	0.393	-0.141	13.502	0.210	1.035	0.399	-0.134	13.805
0.02	12.281	0.201	1.083	0.404	-0.104	14.428	0.190	1.080	0.423	-0.099	14.187
0.03	12.350	0.196	1.270	0.434	-0.105	14.188	0.192	1.265	0.439	-0.103	14.639
0.04	12.379	0.154	1.590	0.532	-0.082	15.124	0.152	1.564	0.536	-0.081	15.019
0.05	12.387	0.137	2.104	0.602	-0.077	14.013	0.115	1.966	0.646	-0.059	15.019
0.06	12.387	0.090	2.642	0.742	-0.063	13.775	0.084	2.357	0.756	-0.057	14.113
0.08	12.363	0.012	3.637	1.009	-0.022	14.261	0.016	2.835	0.996	-0.026	13.436
0.1	12.327	-0.039	4.175	1.239	0.003	12.926	-0.026	3.016	1.189	-0.009	12.522
0.15	12.231	-0.097	4.109	1.555	0.032	13.508	-0.071	2.995	1.431	0.012	16.661
0.2	12.144	-0.114	3.655	1.669	0.040	13.760	-0.086	2.842	1.525	0.019	16.143
0.3	12.028	-0.120	3.057	1.702	0.042	14.173	-0.094	2.597	1.562	0.023	16.939
0.4	11.931	-0.114	2.748	1.653	0.038	14.492	-0.094	2.439	1.544	0.024	15.377
0.5	11.896	-0.108	2.551	1.601	0.037	14.421	-0.090	2.318	1.509	0.024	15.886
0.6	11.924	-0.100	2.415	1.546	0.034	14.579	-0.086	2.223	1.475	0.025	15.290
0.8	11.772	-0.087	2.236	1.453	0.031	14.829	-0.077	2.104	1.405	0.024	15.539
1	11.825	-0.075	2.114	1.380	0.027	15.074	-0.069	2.007	1.351	0.023	15.692
1.5	11.540	-0.053	1.938	1.251	0.020	14.407	-0.049	1.872	1.233	0.017	15.381
2	11.304	-0.035	1.842	1.157	0.013	14.647	-0.034	1.792	1.154	0.012	14.956
3	11.230	-0.010	1.704	1.053	-0.001	11.620	-0.011	1.682	1.058	0.001	11.903
4	11.197	0.008	1.613	0.985	-0.011	13.426	0.006	1.604	0.993	-0.009	12.893
5	11.193	0.021	1.543	0.941	-0.017	12.740	0.018	1.536	0.953	-0.021	14.195
6	11.185	0.024	1.478	0.929	-0.027	15.864	0.030	1.492	0.918	-0.024	11.501
8	11.175	0.033	1.387	0.904	-0.023	12.222	0.033	1.406	0.902	-0.026	13.588
10	11.175	0.035	1.321	0.898	-0.028	14.046	0.043	1.346	0.878	-0.033	13.172
15	11.172	0.042	1.226	0.883	-0.036	14.620	0.063	1.261	0.827	-0.055	14.330

The variation of EABF and EBF for both obsidian samples with incident photon energy at some selected penetration depth is plotted in Figure 7. The EABF and EBF values of both obsidian samples have similar tendency. This is because of the both obsidian specimens have similar chemical components. From this Figure 7, it can be observed that the EABF and EBF values of obsidians are small for all penetration depths at low energies where photoelectric absorption is the dominating photon interaction process and increases with the increase in the incident photon energy. In the intermediate energy region where the Compton scattering dominates EABF and EBF gradually increase and have highest value at 0.2 MeV for the samples. Then EABF and EBF values decrease with increase in photon energy for all penetration depths in the high energy region.

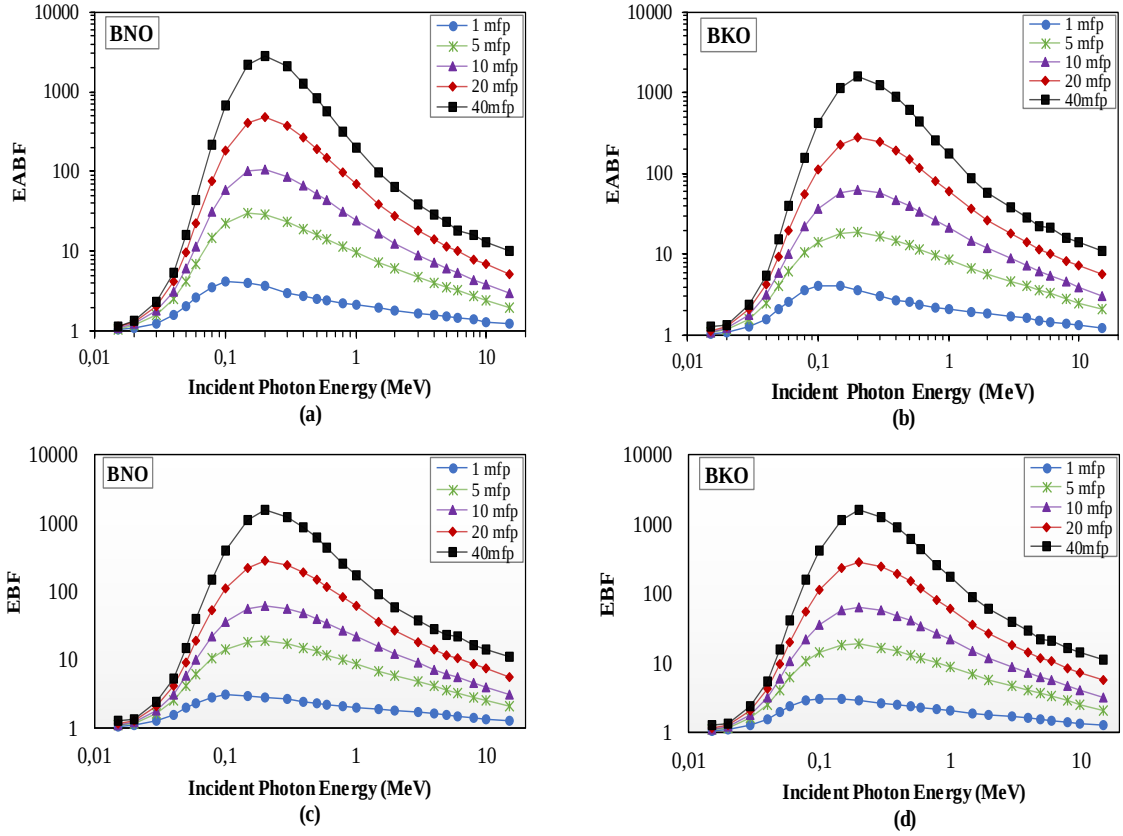

Figure 7. (a-d) EABF and EBF values of the BNO and BKO versus photon energy at different mfps

The variations of EABF and EBF with penetration depth of obsidian specimens for 0.015, 0.15, 1.5 and 15 MeV are given in Figures 8 (a-d) and 9 (a-d), respectively. It is clear from these figures that EABF and EBF values increase with the increase of mean free path values. It was observed that the EABF and EBF values of black obsidian at 0.015 and 0.15 MeV energies are slightly higher than brown obsidian whereas EABF and EBF values obtained for both obsidians at 1.5 and 15 MeV energies are approximately the same.

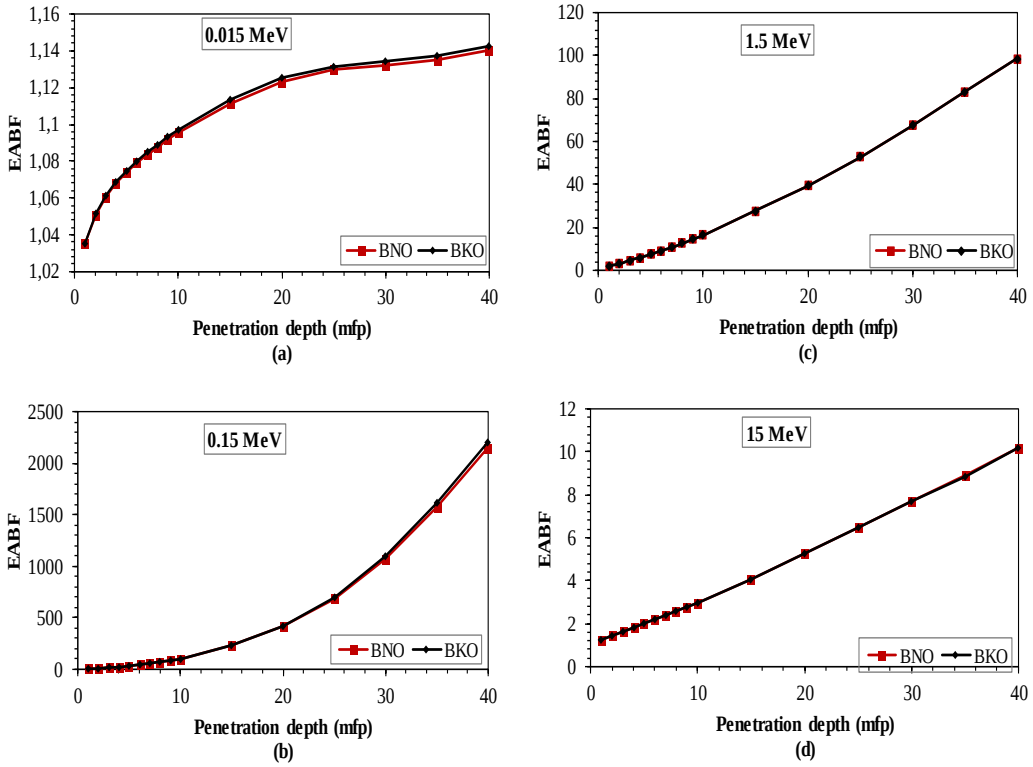

Figure 8. (a-d). The EABF values for obsidian glasses versus the penetration depths at 0.015, 0.15, 1.5, 15 MeV energies.

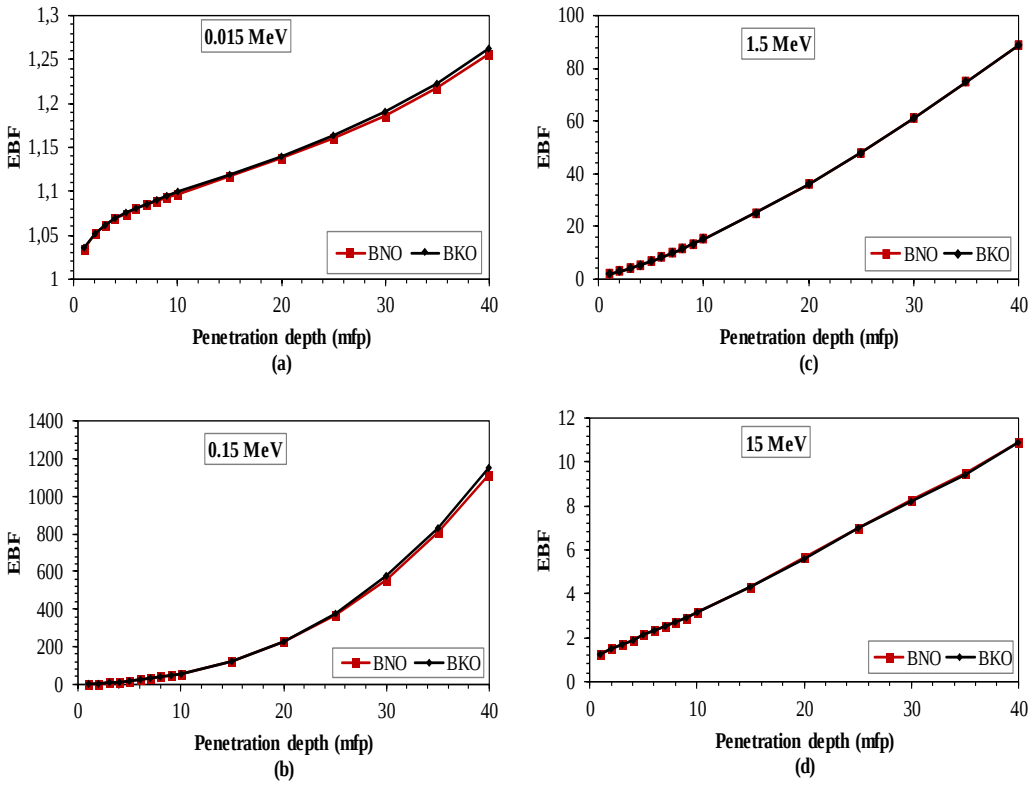

Figure 9. (a–d). EBF values for obsidian glasses up to 40 mfp at 0.015, 0.15, 1.5, 15 MeV.

In addition, our obtained EABF and EBF values are consistent with the results obtained by Küçük and Gezer. They investigated EABF and EBF of black obsidian samples taken from Artvin and Van for 16 types of penetration depth in the energy range from 0.015 to 15 MeV [37].

Table 5 compares EBF values of examined samples with the OC some selected incident photon energies at1 5, 10, 20 and 40 mfp penetration depths. The EBF values of both samples are slightly lower than the OC at 0.15 and 1.5 MeV photon energies for all penetration depths. At 15 MeV photon energy, EBF values of BNO and BKO slightly higher to the values of OC for all penetration depths except 1mfp. At 15 MeV photon energy, EBF values of BNO, BKO and OC very close to the each other for all penetration depths. From these comparisons, it can be concluded that these naturally occurring volcanic glasses can be used for radiation shielding applications especially for low energies.

Table 5. Comparison of EBF values of BNO, BKO and OC

Energy (MeV)	BNO	BKO	OC
EBF for 1 mfp			
0.015	1.035	1.035	1.035
0.15	2.985	2.995	3.000
1.5	1.872	1.872	1.875
15	1.261	1.261	1.263
EBF for 5 mfp			
0.015	1.075	1.076	1.076
0.15	18.044	18.246	18.335
1.5	6.769	6.769	6.786
15	2.100	2,100	2.095
EBF for 10 mfp			
0.015	1.097	1.099	1.098
0.15	56.050	56.979	57.391
1.5	15.079	15.079	15.128
15	3.125	3.124	3.075
EBF for 20 mfp			
0.015	1.137	1.140	1.126
0.15	222.803	227.878	230.139
1.5	36.042	36.042	36.206
15	5.611	5.603	5.305
EBF for 40 mfp			
0.015	1.255	1.262	1.143
0.15	1116.608	1153.794	1170.555
1.5	88.601	88.601	89.285
15	10.912	10.872	9.309

4. CONCLUSION

In this paper, the gamma radiation shielding performance of naturally occurring obsidian glasses are investigated which are taken from the Sarıkamış district of Kars province located at the eastern part of Turkey. The μ, μ_m, mfp, HVL, TVL, Z_{eff} and N_{eff} parameters of these obsidian glasses have been investigated experimentally for the 661.66, 1172.23 and 1332.48 keV gamma ray energies and theoretically computed using the WinXCOM software. The results were compared with the OC commonly used. It was observed that the values of μ, μm, Z_{eff} and N_{eff} of obsidian glasses are quite high at low energies and decreased with increasing gamma ray energy. Also, the μfp, HVL and TVL values of BNO are smaller than the values of BKO and OC at 661.66, 1172.23 and 1332.48 keV gamma energies. The EABF and EBF values of these obsidian specimens were computed using G-P fitting method in the energy range 0.015-15 MeV up to 40 mfp penetration depths and variation of EABF and EBF photon energy and penetration depth were presented graphically. It was observed that EBF values brown obsidian generally less than black obsidian and ordinary concrete. Among the studied samples brown obsidian may be used as a better alternative gamma ray protection material than black obsidian especially for the low energy region.

REFERENCES

[1] Kurudirek M. Heavy metal borate glasses: potential use for radiation shielding. Journal of Alloys and Compounds 2017; 727: 1227-1236.

[2] Kirdsiri K, Kaewkhao J, Pokaipisit A, Chewpraditkul W, Limsuwan P. Gamma-rays shielding properties of xPbO:(100 -x)B2O3 glasses system at 662 keV. Annals of Nuclear Energy 2009; 36: 1360-1365.

[3] Singh T, Kaur A, Sharma J, Singh PS. Gamma rays' shielding parameters for some Pb-Cu binary alloys. Engineering Science and Technology, an International Journal 2018; 21: 1078-1085.

[4] Akkurt I. Effective atomic and electron numbers of some steels at different energies. Annals of Nuclear Energy 2009; 36: 1702–1705.

[5] Alım B, Şakar E, Baltakesmez A, Han İ, Sayyed MI, Demir L. Experimental investigation of radiation shielding performances of some important AISI-coded stainless steels: Part I. Radiation Physics and Chemistry 2019; 160; 108455.

[6] Icelli O, Erzeneoglu S, Karahan IH. Cankaya G. Effective atomic numbers for CoCuNi alloys using transmission experiments. Journal of Quantitative Spectroscopy and Radiative Transfer 2005; 91(4): 485-491.

[7] Han I, Demir L. Studies on effective atomic numbers, electron densities from mass attenuation coefficients in TixCo1-x and CoxCu1-x alloys. Nuclear Instruments and Methods in Physics Research Section B, 2009; 267: 3505–3510.

[8] Şakar E, Büyükyıldız M, Alım B, Şakar BC, Kurudirek M. Leaded brass alloys for gamma-ray shielding applications. Radiation Physics and Chemistry 2019; 159: 64–69.

[9] Akman F, Kaçal MR, Sayyed MI, Karataş HA. Study of gamma radiation attenuation properties of some selected ternary alloys. Journal of Alloys and Compounds 2019; 782: 315–322

[10] Baltas H, Celik S, Cevik U, Yanmaz E. Measurement of mass attenuation coefficients and effective atomic numbers for MgB2 superconductor using X-ray energies. Radiation Measurements 2007; 42: 55-60.

[11] Baltas H, Cevik U, Tırasoglu E, Ertugral B, Apaydın G, Kobya AI. Mass attenuation coefficients of YBaCuO and BiPbSrCaCuO superconductors at 511, 661 and 1274 keV energies. Radiation Measurements 2005; 39: 33–37.

[12] Cevik U, Baltas H. The mass attenuation coefficients and electron densities for BiPbSrCaCuO superconductor at different energies. Nuclear Instruments and Methods in Physics Research Section B 2007; 256: 619–625.

[13] Oto B, Yıldız N, Akdemir F, Kavaz E. Investigation of gamma radiation shielding properties of various ores. Progress in Nuclear Energy 2015; 85: 391-403.

[14] Akkurt I, Basyigit C, Kilincarslan S, Mavi B. The shielding of γ-rays by concretes produced with barite. Progress in Nuclear Energy 2005; 46 (1); 1-11.

[15] Singh K, Singh H, Sharma G, Gerward L, Khanna A, Kumar R, Nathuram R, Sahota HS. Gamma-ray shielding properties of CaO–SrO–B2O3 glasses. Radiation Physics and Chemistry 2005; 72: 225–228.

[16] Gerward L, Guilbert N, Jensen KB, Levring H. WinXCom - a program for calculating X-ray attenuation coefficients. Radiation Physics and Chemistry 2004; 71; 653–654.

[17] Chanthima N, Kaewkhao J. Investigation on radiation shielding parameters of bismuth borosilicate glass from 1 keV to 100 GeV. Annals of Nuclear Energy 2013; 55: 23–28.

[18] Mostafa AMA, Issa SA, Sayyed MI. Gamma ray shielding properties of PbO-B2O3-P 2O5 doped with WO3. Journal of Alloys and Compounds 2017; 708: 294-300.

[19] Sayyed MI, Kaky KM, Şakar E, Akbaba U, Taki MM, Agar O. Gamma radiation shielding investigations for selected germanate glasses. Journal of Non-Crystalline Solids 2019; 512: 33–40.

[20] Ahmed GSM, Mahmoud AS, Salem SM, Abou-Elnasr TZ. Study of Gamma-Ray Attenuation Coefficients of Some Glasses Containing CdO. American Journal of Physics and Applications 2015; 3(4): 112-120.

[21] Cengiz G, Çağlar I, Bilir G. Optical Properties and Natural Radioactivity Levels of Turkish Natural Glass Obsidian. The Eurasia Proceedings of Science Technology Engineering and Mathematics 2019; 6: 138-141.

[22] Çolak A, Aygün H. Sarıkamış (Kars) civarı obsidiyenleri bilgi notu. MTA. Maden Etüt ve Arama Dairesi Başkanlığı SERKA Raporu. Kars, 2011.

[23] https://www.ortec-online.com/products/application-software/maestro-mca (06.11.2020)

[24] Jackson DF, Hawkes DJ. X-ray attenuation coefficients of elements and mixtures. Physics Reports 1981; 70: 169–233.

[25] Elmahroug Y, Tellili B, Souga C. Determination of total mass attenuation coefficients, effective atomic numbers and electron densities for different shielding materials. Annals of Nuclear Energy 2015; 75: 268-274.

[26] Sayyed MI. Bismuth modified shielding properties of zinc boro-tellurite glasses. Journal of Alloys and Compounds 2016; 688: 111–117.

[27] Yorgun NY, Kavaz E. Gamma photon protection properties of some cancer drugs for medical applications. Results in Physics 2019; 13: 102150.

[28] Raut, SD, Awasarmol VV, Shaikh SF, Ghule BG, Ekar SU, Mane RS, Pawar PP. Study of gamma ray energy absorption and exposure buildup factors for ferrites by geometric progression fitting method. Radiation Effects and Defects in Solids 2018; 173: 3-4, 429-438.

[29] Sakar E, Ozpolat OF, Alım B, Sayyed M, Kurudirek M. Phy-X/PSD: Development of a user friendly online software for calculation of parameters relevant to radiation shielding and dosimetry. Radiation Physics and Chemistry 2020: 108496; 1-12.

[30] ANSI/ANS-6.4.3, 1991. Gamma Ray Attenuation Coefficient and Buildup Factors for Engineering Materials. American Nuclear Society La Grange Park, Illions.

[31] Kavaz E, Ahmadishadbad N, Özdemir Y. Photon buildup factors of some chemotherapy drugs. Biomed Pharmacother 2015; 69: 34–41.

[32] Ekinci N. Kavaz E, Aygün B, Perişanoğlu U. Gamma ray shielding capabilities of rhenium-based superalloys, Radiation Effects and Defects in Solids 2019; 174:5-6, 435-451.

[33] Harima Y. An approximation of gamma-ray buildup factors by modified geometrical progression. Nuclear Science and Engineering 1983; 83(2): 299–309.

[34] Bootjomchai C, Laopaiboon L, Yenchai C, Laopaiboon R. Gamma-ray shielding and structural properties of barium–bismuth–borosilicateglasses. Radiation Physics and Chemistry 2012; 81: 785–790.

[35] Singh VP, Badiger NM. Investigation on radiation shielding parameters of ordinary, heavy and super heavy concretes. Nuclear Technology Radiation &Protection 2014; 29 (2); 149-156.

[36] Sayyed MI, Kaky KM, Gaikwad DK, Agar O, Gawai UP, Baki SO. Physical, structural, optical and gamma radiation shielding properties of borate glasses containing heavy metals (Bi2O3/MoO3). Journal of Non-Crystalline Solid 2019; 507: 30–37.

[37] Küçük N, Gezer O. Doğal Siyah Obsidyen Cevherleri İçin Yığılma Faktörlerinin Belirlenmesi. Afyon Kocatepe Üniversitesi Fen ve Mühendislik Bilimleri Dergisi 2017; 17 (031101): 872-880.